

# Discovery of 4,6-Disubstituted Pyrimidine Derivatives as Novel Dual VEGFR2/FGFR1 Inhibitors

Jin-Yang Zhang,<sup>a</sup> Wen-Jun Xue,<sup>a</sup> Min Wang,<sup>a</sup> Wen Li,<sup>a</sup> Ru Dong,<sup>a</sup> Ming-Tao Li,<sup>a</sup> and Li-Ping Sun<sup>\*a</sup>

<sup>a</sup> Jiangsu Key Laboratory of Drug Design and Optimization, Department of Medicinal Chemistry, China Pharmaceutical University, Nanjing 210009, P. R. China, e-mail: chslp@cpu.edu.cn

Abnormalities in the FGFRs signaling pathway and VEGFR2 amplification often occur in a variety of tumors, and they synergistically promote tumor angiogenesis. Studies have shown that the up-regulation of FGF-2 is closely related to the resistance of VEGFR2 inhibitors. Activation of the FGFRs signal is a signal of compensatory angiogenesis after VEGFR2 resistance. Dual VEGFR2/FGFR1 inhibitors contribute to overcoming the resistance of VEGFR2 inhibitors and inhibit tumor growth significantly. Based on this, we designed and synthesized a series of 4,6-disubstituted pyrimidine derivatives as dual VEGFR2/FGFR1 inhibitors by the molecular hybridization strategy. 3-(2,6-Dichloro-3,5-dimethoxyphenyl)-1-{6-[(4-methoxyphenyl)amino]pyrimidin-4-yl}-1-methylurea (**8b**) had the best inhibitory activities against VEGFR2 and FGFR1 at 10  $\mu$ M (82.2% and 101.0%, respectively), it showed moderate antiproliferative activities against A549 and KG-1 cell lines as well. Besides, molecular docking was also carried out to study the binding mode of 3-(2,6-dichloro-3,5-dimethoxyphenyl)-1-{6-[(4-methoxyphenyl)-amino]-pyrimidin-4-yl}-1-methylurea (**8b**) with VEGFR2 and FGFR1. These studies reveal that this series of compounds deserve further optimization.

**Keywords:** VEGFR2, FGFR1, dual inhibitors, 4,6-disubstituted pyrimidine, antitumor activity.

## Introduction

Vascular Endothelial Growth Factor Receptor 2 (VEGFR2) plays a crucial role in promoting angiogenesis and increasing vascular permeability as a receptor tyrosine kinase, and inhibiting VEGFR2 has become an effective strategy for tumor treatment.<sup>[1]</sup> The FDA has approved several small-molecule VEGFR2 inhibitors for tumor treatment, such as Sorafenib,<sup>[2]</sup> Pazopanib,<sup>[3]</sup> and Lenvatinib (*Figure 1*).<sup>[4]</sup> As an increasing number of VEGFR2 inhibitors were used clinically, drug resistance has gradually become prominent.<sup>[5]</sup>

It was reported that FGF-2 overexpression is one of the mechanisms of resistance to VEGFR2 inhibitors.<sup>[6]</sup> Fibroblast Growth Factors (FGFs) are division promoting factors and chemokine in vascular endothelial cells, which can stimulate the migration, proliferation, and differentiation of vascular cells, and have a synergistic

effect with VEGFs in promoting tumor blood vessel growth.<sup>[7]</sup> The activation of FGFs signaling participates in the resistance to VEGFs pathway inhibition (*Figure 2*).<sup>[8]</sup> Among them, FGF-2 plays a particularly prominent role in angiogenesis. FGF-2 is bound to Fibroblast Growth Factor Receptors (FGFRs) and induces endothelial cell proliferation. FGF-2 promotes the expression of VEGF by enhancing the signal of the PI3K pathway, and VEGF also needs to be in the presence of FGF-2 to promote angiogenesis. When VEGF and FGF-2 are expressed simultaneously, the density and permeability of blood vessels will be improved, and blood vessels will grow rapidly.<sup>[9]</sup> Furthermore, alterations of the FGFR gene have been detected in a variety of tumor types.<sup>[10]</sup> FGFR gene alterations and VEGFR up-regulation are commonly found in the same types of cancers, such as lung cancer,<sup>[11,12]</sup> gastric cancer,<sup>[13,14]</sup> and breast cancer.<sup>[15]</sup>

For the above reasons, selective targeting FGFR1 and VEGFR2 has potential therapeutic advantages for tumors, also can overcome VEGFR2 inhibitors resistance. Furthermore, the aberrant tumor vasculature

Supporting information for this article is available on the WWW under <https://doi.org/10.1002/cbdv.202100095>

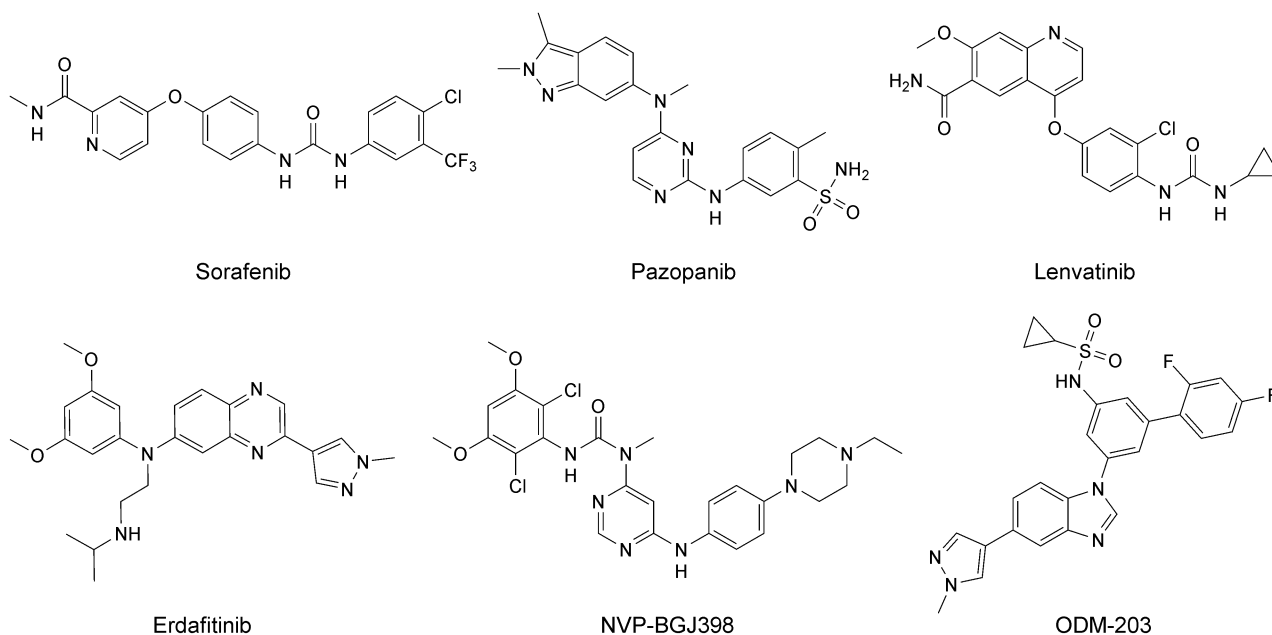


**Figure 1.** Structure of representative VEGFR and FGFR inhibitors.

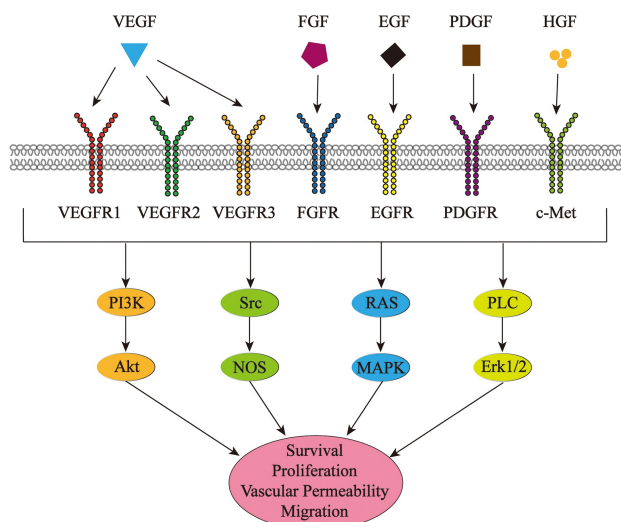
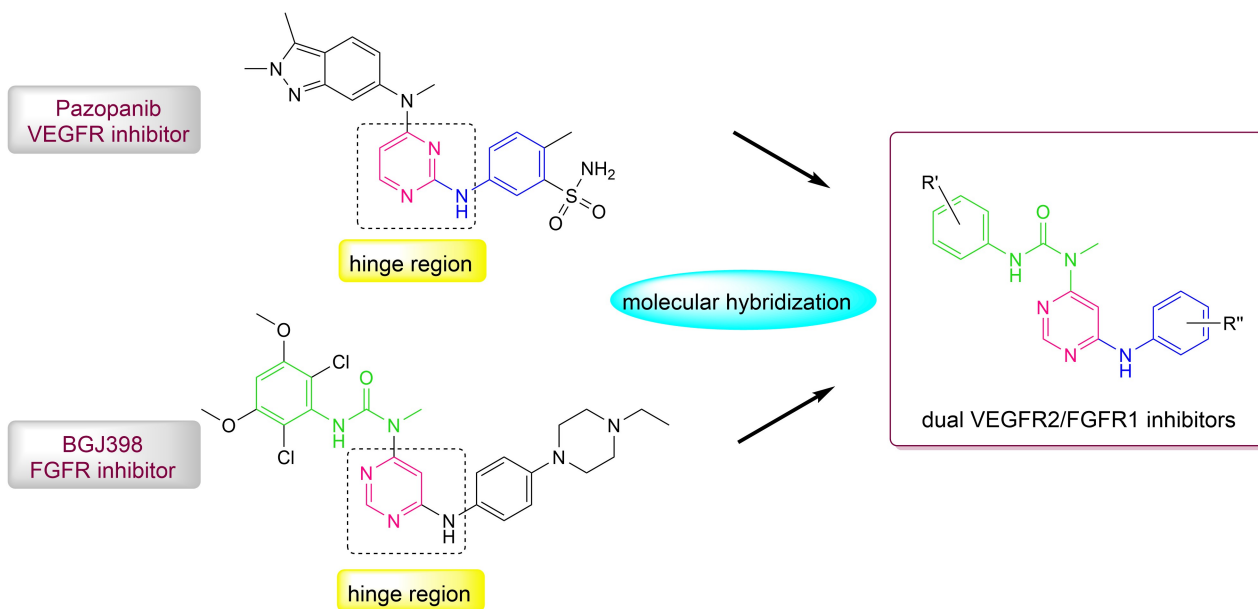


**Figure 2.** VEGFR-FGFR signaling pathways.

mediated by pro-angiogenic factors enhanced tumor potential by supporting immunosuppressive tumor microenvironment to escape host immune surveillance.<sup>[16,17]</sup> Hence targeting the VEGFR and FGFR signaling pathway can also improve the tumor immune microenvironment.<sup>[18]</sup>

At present, several FGFR inhibitors have been approved by the FDA, such as Erdafitinib.<sup>[19]</sup> And some FGFR inhibitors are in clinical studies, such as NVP-BGJ398.<sup>[20]</sup> Besides, ODM-203 has been reported as a

dual VEGFR/FGFR inhibitor (Figure 1).<sup>[18]</sup> To avoid the toxicities and side effects of drug interactions that may be caused by the combination of single-target drugs, we designed a series of dual VEGFR2/FGFR1 inhibitors based on Pazopanib and NVP-BGJ398. Pazopanib, a multitargeted kinase inhibitor, was approved by the FDA in 2009 and 2012 for the treatment of renal cell carcinoma and soft tissue sarcoma, respectively. Its  $IC_{50}$  value is 30 nM for VEGFR2. According to reports, the NH on aniline and the N on pyrimidine formed hydrogen bonds with Cys919 of the hinge region, and benzopyrazole filled the hydrophobic pocket.<sup>[3]</sup> NVP-BGJ398, a potently pan-FGFR inhibitor with a pyrimidine core, inhibited FGFR1-3 with the respective  $IC_{50}$  values of 0.9 nM, 1.4 nM, and 1.0 nM. The cocrystal structure indicated that the NH on the aniline and the N on the pyrimidine formed two key hydrogen bonds with residue Ala564 of the hinge. The 3,5-dimethoxyaniline fragment occupied the hydrophobic pocket, and its O formed a hydrogen bond with Asp641.<sup>[20]</sup> Based on the study of the above binding mode, we designed a series of 4,6-disubstituted pyrimidine derivatives as dual VEGFR2/FGFR1 inhibitors using the molecular hybridization strategy (Scheme 1).



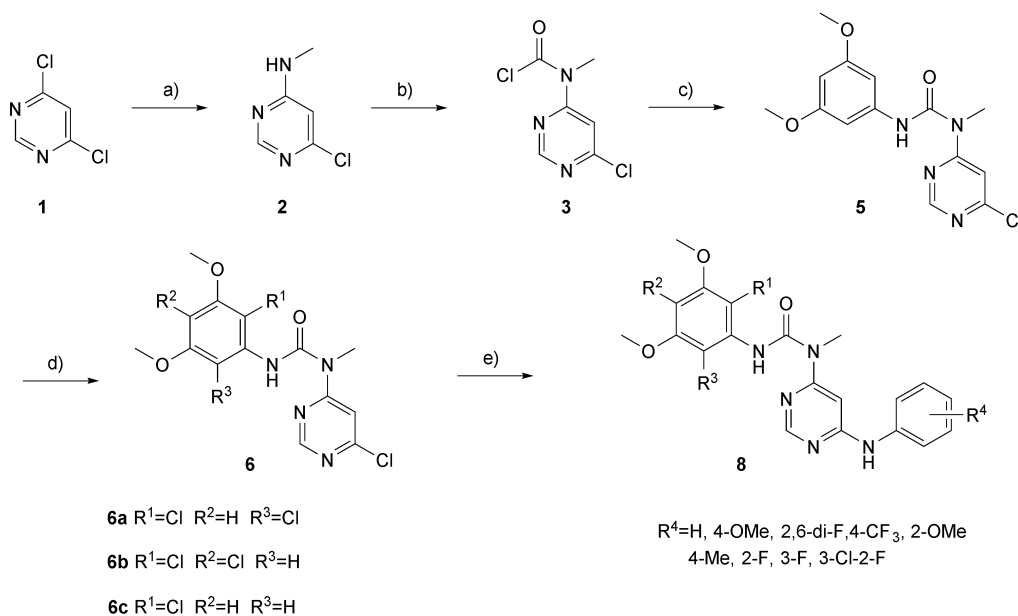
**Scheme 1.** Design of target dual VEGFR2/FGFR1 inhibitors.

## Results and Discussion

### Chemistry

The synthesis route of the target compounds **8a–8t** was outlined in *Scheme 2*. All target compounds were synthesized according to the following route: Using

4,6-dichloropyrimidine (**1**) as the starting material, 4-chloro-6-methylaminopyrimidine (**2**) was prepared by amination reaction with methylamine. The intermediate **2** was acylated by triphosgene (BTC) with pyridine as base to (6-chloropyrimidin-4-yl)(methyl)carbamic chloride (**3**). Then, the intermediate **3** reacted with 3,5-



**Scheme 2.** Synthesis of target compounds **8a–8t**. Reagents and condition: (a) Methylamine in ethanol (30–33%), i-PrOH, r.t., 1 h; (b) BTC, pyridine, dry DCM, 0 °C, 1 h; (c) **4** (3,5-dimethoxyaniline), Et<sub>3</sub>N, dry DCM, 0 °C, 2 h; (d) NCS, dry CH<sub>3</sub>CN, reflux; (e) **7** (anilines), concentrated HCl, i-PrOH, 90 °C, 12 h.

dimethoxyaniline (**4**) in the presence of triethylamine to form 1-(6-chloropyrimidin-4-yl)-3-(3,5-dimethoxyphenyl)-1-methylurea (**5**). The intermediate **5** and NCS were heated to reflux in dry acetonitrile to obtain 1-(6-chloropyrimidin-4-yl)-3-(2,6-dichloro-3,5-dimethoxyphenyl)-1-methylurea (**6a**), 1-(6-chloropyrimidin-4-yl)-3-(2,4-dichloro-3,5-dimethoxyphenyl)-1-methylurea (**6b**), and 3-(2-chloro-3,5-dimethoxyphenyl)-1-(6-chloropyrimidin-4-yl)-1-methylurea (**6c**). Finally, intermediates **6a–6c** were substituted with various anilines (**7**) under the condition of concentrated hydrochloric acid to obtain the target compounds **8a–8t**.

### Kinase Profiling

Based on our previous research, the activities of compounds **8a–8t** against FGFR1 and VEGFR2 were determined at the concentration of 10  $\mu$ M. The results were shown in Table 1. In general, the inhibition rates of the target compounds **8a–8t** on FGFR1 were slightly better than VEGFR2. The inhibition rates of compounds **8a**, **8b**, **8f**, and **8l** for VEGFR2 and FGFR1 were above 60% and 85%, respectively. By analyzing the structure–activity relationship, we found that the position of the chlorine atoms had a great influence on the potency. The compounds with both chlorine substituents at R<sup>1</sup> and R<sup>3</sup> showed good inhibitory activities. When R<sup>4</sup>

was substituted by 4-methyl, the FGFR1 inhibitory activities of compounds **8f**, **8l**, and **8s** were better (99.9%, 86.2%, and 69.6%, respectively), and the VEGFR2 inhibitory activities of **8f** and **8l** were also better (63.1% and 67.8%, respectively). The compounds with R<sup>4</sup> at *para*-position showed good inhibitory activities for VEGFR2. Compound **8b** (R<sup>4</sup> = 4-methoxy, 82.2%) showed better inhibitory activity against VEGFR2 than compound **8e** (R<sup>4</sup> = 2-methoxy, 46.6%). Overall, compound **8b** exhibited the strongest potency against VEGFR2 and FGFR1 (82.2% and 101.0%, respectively), which were comparable to the reference drug Nintedanib (97.7% and 101.1%, respectively).

### Antiproliferative Activity Study

FGFR gene alterations and VEGFR up-regulation were frequently found in lung cancer and breast cancer, so the antiproliferative activities of the compounds were detected in human lung cancer A549 cell lines and human breast cancer MCF-7 cell lines by MTT assays. Besides, we chose the human liver cancer HepG-2 cell lines and leukemia KG-1 cell lines (FGFR1-translocated) for antiproliferation assay by MTT or CCK-8 assays. As shown in Table 2, the compounds showed better activities against A549 cell lines and MCF-7 cell lines than HepG-2 cell lines in general. The compound **8b**

**Table 1.** Kinase inhibition (%; 10  $\mu$ M) against VEGFR2 and FGFR1.

Compound	R <sup>1</sup>	R <sup>2</sup>	R <sup>3</sup>	R <sup>4</sup>	Inhibition % <sup>[a]</sup> at 10 $\mu$ M	
					VEGFR2	FGFR1
<b>8a</b>	Cl	H	Cl	H	81.1	99.8
<b>8b</b>	Cl	H	Cl	4-OMe	82.2	101.0
<b>8c</b>	Cl	H	Cl	2,6-di-F	40.8	100.7
<b>8d</b>	Cl	H	Cl	4-CF <sub>3</sub>	23.5	95.6
<b>8e</b>	Cl	H	Cl	2-OMe	46.6	98.0
<b>8f</b>	Cl	H	Cl	4-Me	63.1	99.9
<b>8g</b>	Cl	H	Cl	2-F	22.0	96.2
<b>8h</b>	Cl	H	Cl	3-F	48.1	103.7
<b>8i</b>	Cl	H	Cl	3-Cl-2-F	42.3	97.6
<b>8j</b>	Cl	Cl	H	H	27.6	41.9
<b>8k</b>	Cl	Cl	H	4-OMe	40.6	81.3
<b>8l</b>	Cl	Cl	H	4-Me	67.8	86.2
<b>8m</b>	Cl	Cl	H	4-CF <sub>3</sub>	< 0	1.6
<b>8n</b>	Cl	Cl	H	2,6-di-F	30.4	47.3
<b>8o</b>	Cl	Cl	H	3-Cl-2-F	31.2	49.3
<b>8p</b>	Cl	H	H	4-CF <sub>3</sub>	< 0	< 0
<b>8q</b>	Cl	H	H	2,6-di-F	8.6	27.2
<b>8r</b>	Cl	H	H	2-OMe	6.0	43.7
<b>8s</b>	Cl	H	H	4-Me	47.3	69.6
<b>8t</b>	Cl	H	H	3-Cl-2-F	16.8	33.9
Nintedanib					97.7	101.1

<sup>[a]</sup> Assays were performed in replicate ( $n = 2$ ).

**Table 2.** *In vitro* antiproliferative activity in different tumor cell lines.

Compound	Antitumor cell proliferation				
	A549 (IC <sub>50</sub> , <sup>[a]</sup> μM)	MCF-7 (IC <sub>50</sub> , μM)	HepG-2 (IC <sub>50</sub> , μM)	KG-1 (% at 10 μM)	(% at 1 μM)
<b>8a</b>	> 200	> 200	> 200	70.6	65.1
<b>8b</b>	28.4 ± 6.3	149.1 ± 7.6	> 200	70.0	67.0
<b>8d</b>	56.9 ± 8.2	106.3 ± 15.2	N.A. <sup>[b]</sup>	–	–
<b>8f</b>	45.8 ± 5.9	176.8 ± 36.9	> 200	79.5	74.0
<b>8g</b>	18.9 ± 6.0	56.0 ± 7.9	90.6 ± 10.2	–	–
<b>8h</b>	> 200	57.7 ± 22.8	> 200	71.7	54.4
<b>8i</b>	92.6 ± 31.7	> 200	> 200	67.8	18.6
<b>8j</b>	28.2 ± 0.6	23.2 ± 3.2	46.0 ± 2.6	–	–
<b>8k</b>	51.3 ± 6.0	11.0 ± 1.5	21.2 ± 2.8	23.5	11.7
<b>8l</b>	22.8 ± 9.2	113.6 ± 6.4	> 200	23.6	7.1
<b>8s</b>	> 200	83.4 ± 19.5	> 200	28.9	15.7
Nintedanib	2.8 ± 0.5	2.4 ± 0.8	4.7 ± 0.2	74.9	71.3

<sup>[a]</sup> Results are expressed as Mean ± SD from three independent experiments. <sup>[b]</sup> No activity. –, not tested.

exhibited a moderate antiproliferative effect on A549 cell lines (IC<sub>50</sub> = 28.4 ± 6.3 μM), although it had both good potencies against VEGFR2 and FGFR1. Moreover, the inhibition rate of compound **8b** against KG-1 cell lines was 70.0% at 10 μM, which was similar to the reference drug Nintedanib (74.9% at 10 μM). Although **8k** and **8g** showed only medium potency against VEGFR2, compound **8k** had a better antiproliferative activity for MCF-7 cell lines (IC<sub>50</sub> = 11.0 ± 1.5 μM), and compound **8g** had a better antiproliferative activity for A549 cell lines (IC<sub>50</sub> = 18.9 ± 6.0 μM). Therefore, compound **8b** was selected for subsequent molecular docking studies.

### Molecular Docking

We clarified the binding mode of the effective inhibitor **8b** with VEGFR2 and FGFR1 by molecular docking. As shown in Figure 3, compound **8b** could bind closely to FGFR1 through three hydrogen bonds, one cation-π interaction, several electrostatic interactions, and many Van der Waals interactions. The 3,5-dimethoxyaniline fragment of **8b** occupied a hydrophobic pocket, formed a cation-π interaction with the Lys514 residue. At the same time, one of the O of the methoxy group formed a hydrogen bond with the Asp641 residue (2.6 Å). The NH of aniline and the N of pyrimidine formed two key hydrogen bonds with the Ala564 residue in the hinge region of FGFR1 (2.4 Å and 2.6 Å, respectively). Besides, the docking results showed that two hydrogen bonds and several electrostatic interactions were formed between **8b** and VEGFR2. The NH of aniline and the N of pyrimidine formed two key hydrogen bonds with the

Cys919 residue in the hinge region of VEGFR2 (2.2 Å and 2.2 Å, respectively), and the 4-methoxyaniline fragment of **8b** forming a π-π stacking interaction with the Phe918 residue. The molecular docking results showed that the interaction between compound **8b** and FGFR1 was more strongly than that between compound **8b** and VEGFR2, which could explain that the inhibition activity of the compounds **8b** against FGFR1 was slightly better than the activity of VEGFR2. In general, molecular docking showed that compound **8b** could bind to VEGFR2 and FGFR1 tightly. The specific structure-activity relationship was shown in Figure 4.

### Conclusions

In summary, we designed and synthesized a series of 4,6-disubstituted pyrimidine derivatives as novel dual VEGFR2/FGFR1 inhibitors, and then, evaluated their VEGFR2/FGFR1 inhibitory activities and tumor cell antiproliferation activities *in vitro*. Most of them showed good potency against FGFR1 and VEGFR2 and moderate antiproliferative activities. The inhibition rates of **8b** against VEGFR2 and FGFR1 were 82.2% and 101.0% at 10 μM, respectively. Besides, antiproliferation assay *in vitro* showed that compound **8b** had moderate inhibitory activity against human lung cancer A549 cell lines with an IC<sub>50</sub> of 28.4 μM. Furthermore, molecular docking explained the interactions of **8b** with the VEGFR2 and FGFR1. Our results would provide the basis for the design and discovery of new dual VEGFR2/FGFR1 inhibitors.

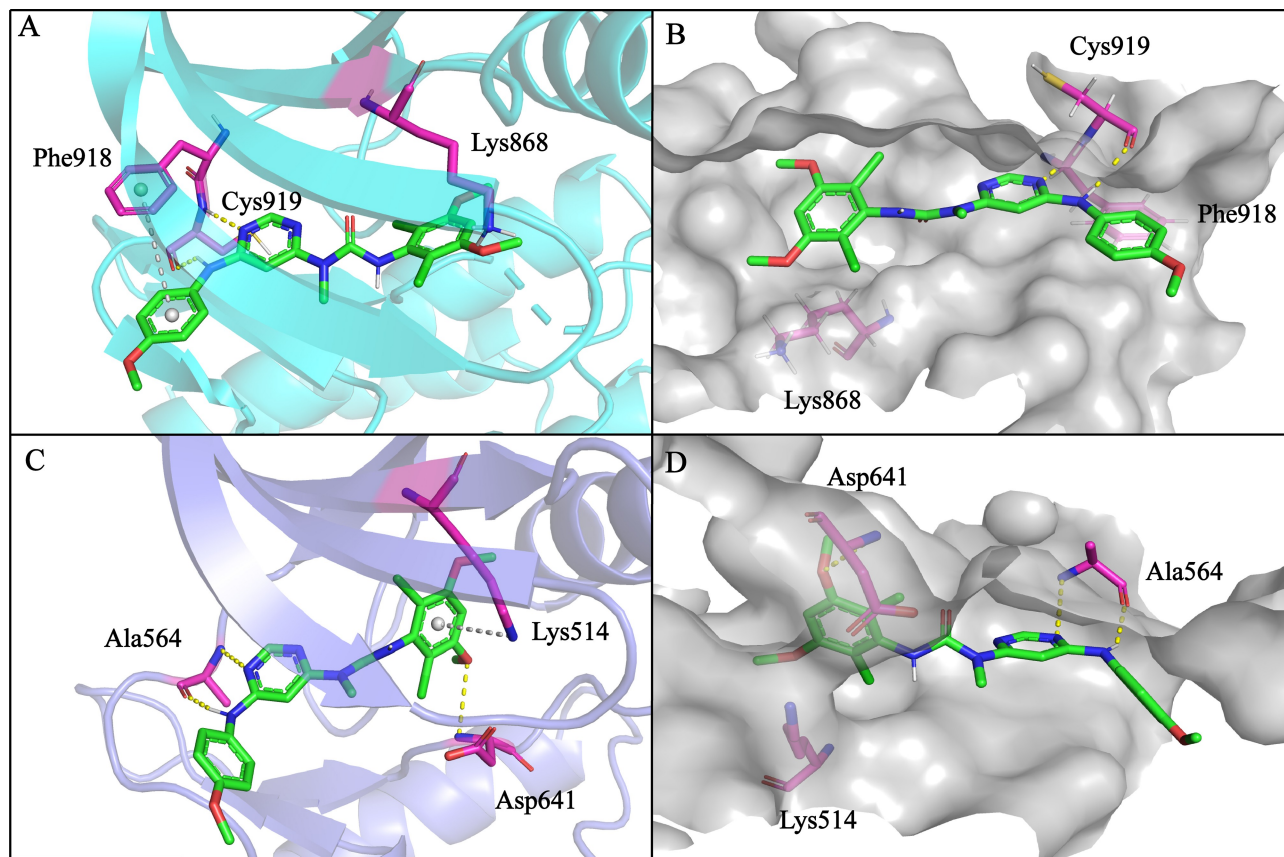


**Figure 3.** The docking model of compound **8b** with VEGFR2 and FGFR1. The hydrogen bonds are displayed as yellow dotted lines. (A) 3D model of **8b** bound to VEGFR2 (PDB code: 3CJF). (B) Compound **8b** bound to the ATP binding pocket of VEGFR2. (C) 3D model of **8b** bound to FGFR1 (PDB code: 3TT0). (D) Compound **8b** bound to the ATP binding pocket of FGFR1.

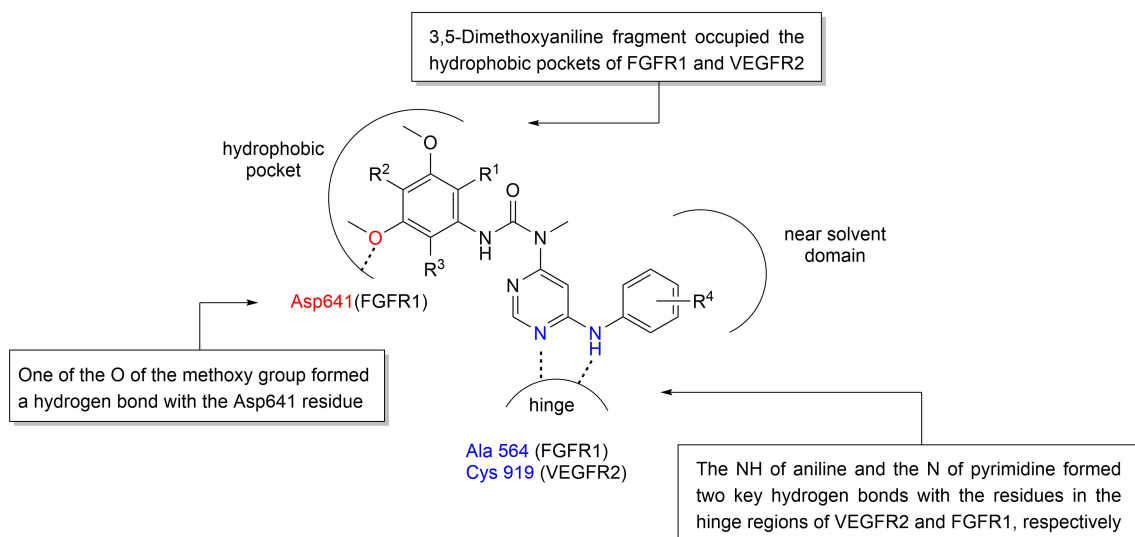


**Figure 4.** SAR of compound **8**.

## Experimental Section

### Chemical Synthesis

The materials involved were purchased from commercial suppliers, the reagents and solvents are analytically graded and can be used directly without further purification. All reactions were monitored by thin-layer chromatography (TLC) (purchased from Qingdao Marine Chemical Plant). Flash column chromatography was performed with silica gel (200–300 mesh, purchased from Qingdao Marine Chemical Plant).  $^1\text{H}$ - and  $^{13}\text{C}$ -NMR spectra were determined in ( $\text{D}_6$ )DMSO or  $\text{CDCl}_3$  solutions using the Bruker AV-300 spectrometer. Q-tof high-resolution mass spectrometer was used for mass spectrometry analysis. The melting points were measured on the RY-1 MP device. The IR spectra were recorded on a Nicolet iS10 infrared spectrometer.

### 6-Chloro-*N*-methylpyrimidin-4-amine (2)

4,6-Dichloropyrimidine (3.45 g, 24 mmol) and 60 mL isopropanol were added to a reaction bottle, stirred, and 18 mL methylamine ethanol solution was slowly added to the reaction bottle. The reaction solution was stirred for 1 h at room temperature. After the reaction was completed, the reaction solution was concentrated under reduced pressure. Next, purification of the crude residue by flash column chromatography on silica gel (ethyl acetate/petroleum ether 4:1) afforded the white **2** (3.18 g, 92.3%).

### (6-Chloropyrimidin-4-yl)methylcarbamic Chloride (3)

In the atmosphere of nitrogen, triphosphamide (4 mmol, 1.18 g) was added to the flask, and 20 mL dry DCM was added for stirring and dissolving. Anhydrous pyridine (8 mmol, 1.5 mL) was slowly added in an ice bath. After the drip was completed, compound **2** (8 mmol, 1.15 g) in DCM was slowly added to the flask. After stirring for 1 h in an ice bath, 10% diluted hydrochloric acid was added and stirred for 5 min. Then, 40 mL DCM was used to extract the organic phase 3 times. The organic phase was washed with brine, combined, dried by  $\text{Na}_2\text{SO}_4$ , and then, concentrated.

### 1-(6-Chloropyrimidin-4-yl)-3-(3,5-dimethoxyphenyl)-1-methylurea (5)

Compound **4** (3.2 mmol, 489.9 mg) was added to a two-neck flask, and 15 mL dry DCM solution was

added to stir and dissolve under the ice bath protected by nitrogen, then, the dry DCM solution of compound **3** prepared in the previous step was added slowly. After the addition, dry triethylamine (8 mmol, 1.2 mL) was added to the mixture slowly and stirred in the ice bath for 1 h. At the end of the reaction, 10% diluted hydrochloric acid was added and stirred for 5 min, followed by DCM extraction (40 mL  $\times$  3). The organic phase was washed with brine, combined, and dried over  $\text{Na}_2\text{SO}_4$ . After filtration and concentration in vacuo, the residues were purified by silica gel flash chromatography (DCM/methanol 400:1) to the obtained white solid **5** with a two-step yield of 25.3% in total.

### 1-(6-Chloropyrimidin-4-yl)-3-(2,6-dichloro-3,5-dimethoxyphenyl)-1-methylurea (6a) and 1-(6-Chloropyrimidin-4-yl)-3-(2,4-dichloro-3,5-dimethoxyphenyl)-1-methylurea (6b)

Compound **5** (1.5 mmol, 483.1 mg) was added to the flask. Under the nitrogen atmosphere, dry acetonitrile was added to the flask for stirring and dissolution. Then, the solution of NCS (6 mmol, 801 mg) in DCM was slowly added and refluxed at 80 °C for 1.5 h. The mixture was washed with brine, combined, and dried over  $\text{Na}_2\text{SO}_4$ . After filtration and concentration in vacuo, the residues were purified by silica gel flash chromatography (petroleum ether/ethyl acetate/DCM 8:1:1) to give **6a** (330 mg, 56.4%) and **6b** (250 mg, 42.7%).

### 3-(2-Chloro-3,5-dimethoxyphenyl)-1-(6-chloropyrimidin-4-yl)-1-methylurea (6c)

Compound **5** (0.5 mmol, 161 mg) was added to the flask. Under the nitrogen atmosphere, dry acetonitrile was added to the flask for stirring and dissolution. Then, a solution of NCS (0.6 mmol, 80.2 mg) in DCM was slowly added and heated to 80 °C for 5 h. The mixture was washed with brine, collect the organic phase, and dried over  $\text{Na}_2\text{SO}_4$ . After filtration and concentration in vacuo, the residues were purified by silica gel flash chromatography (petroleum ether/DCM 10:1) to give **6c** (86 mg, 48.3%).

### 3-(2,6-Dichloro-3,5-dimethoxyphenyl)-1-methyl-1-[6-(phenylamino)pyrimidin-4-yl]urea (8a)

Compounds **6a** and **7a** (aniline) were successively added to a reaction tube containing 2 ml isopropanol and stirred. Then, 3 drops of concentrated

hydrochloric acid were added and heated to 90 °C overnight. The reaction solution was concentrated under reduced pressure and dissolved in DCM again. The mixture was washed with brine, combined organic phase, and dried over Na<sub>2</sub>SO<sub>4</sub>. After filtration and concentration in vacuo, the residues were purified by TLC on silica gel (DCM/methanol 80:1) to give **8a** as pale yellow solid (5 mg, 11.2%). The preparation of the other title compounds (**8b–8t**) was accomplished by a similar synthetic procedure. All the spectroscopic data of all the compounds can be found in *Supporting Information*.

#### *In vitro* Kinase Assay

The potencies of the compounds against VEGFR2 and FGFR1 were measured using the caliper mobility shift assay *in vitro*. All compounds were separately dissolved in DMSO to prepare the solution with a concentration of 10 mM.

Preparation of source plate: The compounds were diluted to 50 times of the final desired maximum inhibitory concentration in DMSO, and transferred 100 µL of this solution to the wells of a 96-well plate. Took 100 µL of pure DMSO and added it to two vacant wells of the same 96-well plate as a no enzyme control and a no compound control. The plate was a source plate.

Preparation of intermediate plate: Took 10 µL of the compound solution in the source plate and transferred it to an intermediate plate, it was a new 96-well plate. Took 90 µL of kinase base buffer and add it to each well of the intermediate plate. Shaked the compounds in the intermediate plate for 10 min.

Preparation of assay plate: In duplicate, took 5 µL of liquid from each well of the intermediate plate and transferred it to a new 384-well plate as an assay plate.

Kinase reaction: Added kinase, FAM-labeled peptide, and ATP in kinase base buffer in sequence. 5 µL of compounds were already present in the 10% DMSO of the assay plate. Took 10 µL of 2.5 times enzyme solution and added it to each well of the assay plate. Incubated at 25 °C for 10 min. Then, took 10 µL of 2.5 times peptide solution and added it to each well of the assay plate. Incubated at 28 °C for a while. Took 25 µL of stop buffer and added it to each well to stop the reaction.

Caliper reading: Read and collected data on Caliper. Converted the converted values to inhibition rates. Percent inhibition = (max–conversion)/(max–min) × 100, where 'max' stands for DMSO control and 'min' stands for low control.

#### *Cell Proliferative Assay*

The antiproliferative activities of the compounds against A549, MCF-7, and HepG-2 cells were evaluated by MTT assay. The cells (A549, MCF-7, and HepG-2) at the logarithmic growth stage were inoculated in a 96-well plate with 4000 cells per well and incubated at 5% CO<sub>2</sub> and 37 °C for 24 h. After adherent to the wall, the cells were cultured for 72 h at CO<sub>2</sub> and 37 °C in different concentration of compounds (10<sup>-3</sup> µM, 10<sup>-2</sup> µM, 10<sup>-1</sup> µM, 10 µM, 10<sup>2</sup> µM). The supernatant was discarded, and the serum-free medium containing 0.5 mg/mL MTT of fresh preparation was added to each well with 20 µL. After the cultivation, the supernatant was discarded and 150 µL DMSO was added to dissolve the MTT precipitate per well. After it was oscillated and mixed on a micro oscillator, the optical density was measured at a wavelength of 570 nm on a microplate reader.

The antiproliferative activities of the compounds against KG-1 cells were evaluated by CCK-8 assay. The cells were digested and counted, and 3.0 × 10<sup>4</sup> cells per mL cell suspension were prepared. The 100 µL cell suspension was added to each well of the 96-well plate and incubated at 5% CO<sub>2</sub> and 37 °C for 24 h. Dilute the concentration of the compounds to 10 µM, add 100 µL corresponding drug-containing medium to each well, then, the cells were cultured for 72 h at CO<sub>2</sub> and 37 °C. The 10 µL CCK-8 was added to each well and incubated for 2 h. After it was oscillated and mixed on a micro oscillator, the optical density was measured at a wavelength of 450 nm on a microplate reader.

#### *Molecular Docking*

Molecular docking of the compound **8b** into the X-ray structure of VEGFR2 (PDB code: 3CJF) and FGFR1 (PDB code: 3TT0) were carried out using the Maestro 11.8, respectively. The crystal structure of VEGFR2 and FGFR1 were downloaded from RCSB Protein Data Bank. Unless otherwise specified, the default parameter settings were used. The steps of the docking process are as follows: 1) Preparation of protein: Proteins prepared using the tool of Protein Preparation

Wizard in Maestro 11.8. The missing atoms and polar hydrogens were added. Automatically optimized hydroxy, Asn, Gln, and His states using ProtAssign in the H-bond assignment. Deleted all water molecules. The force field applied OPLS3e. 2) Receptor grid generation: The whole protein was defined as the receptor and the ATP binding site of the kinase was selected as the binding site. The grid box was centered on the ligand and defined to dock ligands similar in size to the workspace ligand. 3) Preparation of ligand: Compounds were processed using LigPrep of the Maestro 11.8 with default settings. 4) Molecular docking: Molecular docking was performed by Ligand Docking of Glide. After the molecular docking, the types of protein–ligand interaction were analyzed. The image files were generated using pymol.

## Acknowledgments

The authors appreciate the financial support from the State Key Laboratory for the Chemistry and Molecular Engineering of Medicinal Resources of Guangxi Normal University (CMEMR2014-CMEMR2018).

## Author Contribution Statement

Jin-Yang Zhang and Wen-Jun Xue designed and synthesized these compounds and wrote the article. Ru Dong, Ming-Tao Li, Min Wang, and Wen Li performed the experiments, analyzed the data, and Li-Ping Sun designed and conceived the experiments.

## References

- [1] G. Limaverde-Sousa, C. Sternberg, C. G. Ferreira, 'Antiangiogenesis beyond VEGF inhibition: a journey from antiangiogenic single-target to broad-spectrum agents', *Cancer Treat. Rev.* **2014**, *40*, 548–557.
- [2] L. Adnane, P. A. Trail, I. Taylor, S. M. Wilhelm, 'Sorafenib (BAY 43-9006, Nexavar), a dual-action inhibitor that targets RAF/MEK/ERK pathway in tumor cells and tyrosine kinases VEGFR/PDGFR in tumor vasculature', *Methods Enzymol.* **2006**, *407*, 597–612.
- [3] P. A. Harris, A. Bolor, M. Cheung, R. Kumar, R. M. Crosby, R. G. Davis-Ward, A. H. Epperly, K. W. Hinkle, R. N. Hunter, J. H. Johnson, 'Discovery of 5-[[4-[(2,3-dimethyl-2H-indazol-6-yl)methylamino]-2-pyrimidinyl]amino]-2-methyl-benzene-sulfonamide (Pazopanib), a novel and potent vascular endothelial growth factor receptor inhibitor', *J. Med. Chem.* **2008**, *51*, 4632–4640.
- [4] J. Matsui, Y. Funahashi, T. Uenaka, T. Watanabe, A. Tsuruoka, M. Asada, 'Multi-kinase inhibitor E7080 sup-
- presses lymph node and lung metastases of human mammary breast tumor MDA-MB-231 via inhibition of vascular endothelial growth factor-receptor (VEGF-R) 2 and VEGF-R3 kinase', *Clin. Cancer Res.* **2008**, *14*, 5459–5465.
- [5] N. Ferrara, 'Pathways mediating VEGF-independent tumor angiogenesis', *Cytokine Growth Factor Rev.* **2010**, *21*, 21–26.
- [6] D. Ribatti, A. Vacca, M. Rusnati, M. Presta, 'The discovery of basic fibroblast growth factor/fibroblast growth factor-2 and its role in haematological malignancies', *Cytokine Growth Factor Rev.* **2007**, *18*, 327–334.
- [7] A. Bikfalvi, S. Klein, G. Pintucci, D. B. Rifkin, 'Biological roles of fibroblast growth factor-2', *Endocrine Reviews* **1997**, *18*, 26–45.
- [8] O. Casanovas, D. J. Hicklin, G. Bergers, D. Hanahan, 'Drug resistance by evasion of antiangiogenic targeting of VEGF signaling in late-stage pancreatic islet tumors', *Cancer Cell* **2005**, *8*, 299–309.
- [9] S. Javerzat, P. Auguste, A. Bikfalvi, 'The role of fibroblast growth factors in vascular development', *Trends Mol. Med.* **2002**, *8*, 483–489.
- [10] M. Touat, E. Ileana, S. Postel-Vinay, F. Andre, J. C. Soria, 'Targeting FGFR Signaling in Cancer', *Clin. Cancer Res.* **2015**, *21*, 2684–2694.
- [11] E. Carrillo de Santa Pau, F. C. Arias, E. Caso Pelaez, G. M. Munoz Molina, I. Sanchez Hernandez, I. Muguruza Trueba, R. Moreno Balsalobre, S. Sacristan Lopez, A. Gomez Pinillos, M. del Val Toledo Lobo, 'Prognostic significance of the expression of vascular endothelial growth factors A, B, C, and D and their receptors R1, R2, and R3 in patients with non-small cell lung cancer', *Cancer* **2009**, *115*, 1701–1712.
- [12] N. Cihoric, S. Savic, S. Schneider, I. Ackermann, M. Bichsel-Naef, R. A. Schmid, D. Lardinois, M. Gugger, L. Bubendorf, I. Zlobec, 'Prognostic role of FGFR1 amplification in early-stage non-small cell lung cancer', *Br. J. Cancer* **2015**, *110*, 2914–2922.
- [13] S. Juttner, C. Wissmann, T. Jons, M. Vieth, J. Hertel, S. Gretschel, P. M. Schlag, W. Kemmner, M. Hocker, 'Vascular endothelial growth factor-D and its receptor VEGFR-3: two novel independent prognostic markers in gastric adenocarcinoma', *J. Clin. Oncol.* **2006**, *24*, 228–240.
- [14] H. Murase, M. Inokuchi, Y. Takagi, K. Kato, K. Kojima, K. Sugihara, 'Prognostic significance of the co-overexpression of fibroblast growth factor receptors 1, 2 and 4 in gastric cancer', *Mol. Clin. Oncol.* **2014**, *2*, 509–517.
- [15] S. Ghosh, C. A. W. Sullivan, M. P. Zerkowski, A. M. Molinaro, D. L. Rimm, R. L. Camp, G. G. Chung, 'High levels of vascular endothelial growth factor and its receptors (VEGFR-1, VEGFR-2, neuropilin-1) are associated with worse outcome in breast cancer', *Hum. Pathol.* **2008**, *39*, 1835–1843.
- [16] Y. Huang, S. Goel, D. G. Duda, D. Fukumura, R. K. Jain, 'Vascular normalization as an emerging strategy to enhance cancer immunotherapy', *Cancer Res.* **2013**, *73*, 2943–2948.
- [17] C. Salem, M. Yosra, C. Sophie, E. Bernard, H. Meriem, N. M. Zaeem, 'Hypoxia Promotes Tumor Growth in Linking Angiogenesis to Immune Escape', *Front. Immunol.* **2012**, *3*, 21–30.
- [18] T. H. Holmstrom, A. M. Moilanen, T. Ikonen, M. L. Bjorkman, T. Linnanen, G. Wohlfahrt, S. Karlsson, R. Oksala, T. Korjamo, S. Samajdar, S. Rajagopalan, S. Chelur, K. Narayanan, R. K.

Ramachandra, J. Mani, R. Nair, N. Gowda, T. Anthony, S. Dhodheri, S. Mukherjee, R. K. Ujjinamatada, N. Srinivas, M. Ramachandra, P. J. Kallio, 'ODM-203, a Selective Inhibitor of FGFR and VEGFR, Shows Strong Antitumor Activity, and Induces Antitumor Immunity', *Mol. Cancer Ther.* **2019**, *18*, 28–38.

[19] A. Markham, 'Erdafitinib: First Global Approval', *Drugs* **2019**, *79*, 1017–1021.

[20] V. Guagnano, P. Furet, C. Spanka, V. Bordas, D. G. Porta, 'Discovery of 3-(2,6-dichloro-3,5-dimethoxy-phenyl)-1-[4-

(4-ethyl-piperazin-1-yl)-phenylamino]-pyrimidin-4-yl]-1-methyl-urea (NVP-BGJ398), a potent and selective inhibitor of the fibroblast growth factor receptor family of receptor tyrosine kinase', *J. Med. Chem.* **2011**, *54*, 7066–7083.

Received February 5, 2021

Accepted April 6, 2021